Available online at www.sciencedirect.com
ScienceDirect
Nuclear Engineering and Design 238 (2008) 178–187
Nuclear Engineering and Design
www.elsevier.com/locate/nucengdes

Flow and pressure drop fluctuations in a vertical tube subject to low frequency oscillations

Rajashekhar Pendyala, Sreenivas Jayanti, A.R. Balakrishnan *

Department of Chemical Engineering, Indian Institute of Technology Madras, Chennai 600036, India

Received 10 January 2007; received in revised form 15 June 2007; accepted 19 June 2007

Abstract

Heat transfer and other equipment mounted on off-shore platforms may be subjected to low frequency oscillations. The effect of these oscillations, typically in the frequency range of 0.1–1 Hz, on the flow rate and pressure drop in a vertical tube has been studied experimentally in the present work. A 1.75 m-long vertical tube of inner diameter 0.016 m was mounted on a plate and the whole plate was subjected to oscillations in the vertical plane using a mechanical simulator capable of providing low frequency oscillations in the range of 8–30 cycles/min at an amplitude of 0.125 m. The effect of the oscillations on the flow rate and the pressure drop has been measured systematically in the Reynolds number range 500–6500. The induced flow rate fluctuations were found to be dependent on the Reynolds number with stronger fluctuations at lower Reynolds numbers. The effective friction factor, based on the mean pressure drop and the mean flow rate, was also found to be higher than expected. Correlations have been developed to quantify this Reynolds number dependence.

1. Introduction

In recent years, there has been a growing interest in a barge-mounted floating nuclear desalination plant to provide potable water in coastal areas. Such plants are cost effective when compared to land-based nuclear power plants, have lesser construction periods and the potential to shift to any place, and have simplified anti-seismic design measures and decommissioning technology (Humphries and Davies, 1998; Panov et al., 1998).

The main difference from a fluid mechanics point of view between a land-based and barge-mounted equipment is the influence of sea wave oscillations on the latter. The thermal hydraulic behavior of barge-mounted equipment is influenced by different motions such as heaving, rolling and pitching (Fig. 1). These oscillations render the flows and processes unsteady. The resulting fluctuations in the flow rate and pressure drop may induce flow instabilities in equipment involving phase change and may have deleterious effect on their performance. There have been a number of previous studies of flows in oscillating conditions. An oscillating environment changes the effective gravity and as a result generates periodic pressure gradients in the system. A considerable amount of analytical and experimental work has been done to understand the nature of oscillating or pulsating flow in a pipe under the influence of periodic pressure fluctuations. Two types of pressure fluctuations have been distinguished: a pulsating flow which is composed of a steady component with a superimposed periodical time-varying oscillating component, and an oscillating flow which only has a time-varying component and has no net flow. Richardson and Tyler (1930) were among the first to measure the cross-sectional velocity distribution in an oscillatory pipe flow. They found that the maximum axial velocity in oscillatory flow occurred near the wall rather than at the center of the pipe as in the case of unidirectional steady flow in a pipe. The overshoot in velocity near the wall, now called Richardson's annular effect, has been verified by Sexl (1930), Womersley (1955) and Uchida (1956) using theoretical analysis of a flow driven by sinusoidal and non-sinusoidal pressure gradient in a fully developed pulsating flow in a pipe. Sexl (1930) developed an analytical solution to the oscillating flow and Uchida (1956) reworked Sexl's oscillatory pressure gradient flow by superimposing the oscillations on a constant pressure gradient. Womersley (1955) showed that, in oscillatory flows, the interaction between viscous and inertial effects would alter the velocity profile so that flow would not be similar to the parabolic shape of a steady laminar flow.

* Corresponding author. Tel.: +91 44 2257 4154; fax: +91 44 2257 0509.
E-mail address: arbala@iitm.ac.in (A.R. Balakrishnan).

0029-5493/$ – see front matter © 2007 Elsevier B.V. All rights reserved.
doi:10.1016/j.nucengdes.2007.06.010

Nomenclature

a	acceleration (m/s^2)
A	radius of rotating disc (m)
D	diameter of pipe (m)
f_{os}	mean friction factor in oscillation
f_{th}	theoretical friction factor
g	gravitational acceleration (m/s^2)
h	height (m)
Re	Reynolds number
ΔRe	magnitude of variation in Re
t	time (s)
u	average liquid velocity (m/s)
Δu	magnitude of variation in average liquid velocity (m/s)
v	velocity (m/s)
$\Delta \bar{v}$	magnitude of variation in flow rate (m^3/s)
x	displacement (m)
x_L	entrance length (m)
X	length between center of rotating disc and test section frame (m)
Z	length of connecting rod (m)

Greek letters

α	magnitude of acceleration ($A\omega^2$) (m/s^2)
β	beta ratio
ν	kinematic viscosity (m^2/s)
θ	angle of rotation (rad)
ρ	density (kg/m^3)
ω	angular frequency of oscillation (rad/s)
$\sqrt{\omega'}$	dimensionless frequency parameter
Ψ	fraction of magnitude of flow variation to the mean flow

Gündoğdu and Çarpinlioğlu (1999, 2001) reviewed the available literature up to 2001 on pulsatile flow in detail. They reported that experimental results indicated that the addition of oscillations to steady flow increased the flow resistance. However, the effect of oscillation amplitude on flow resistance is not clear. Hershey and Song (1967) reported in their experiments that the time-averaged friction factors while pulsating were greater than those of steady flow. Claman and Minton (1977) presented a theoretical and experimental study of an oscillating vertical pipe with down flow, in which velocity distribution across the radius and the onset of turbulence were investigated. They solved the transient axial momentum equation with a sinusoidal pressure gradient and obtained the velocity variation in terms of Bessel functions. The predicted velocity profiles in the oscillating boundary layer near the pipe wall were found to agree well at low Reynolds numbers with experimental results obtained using the hydrogen bubble technique. However, at higher Reynolds numbers the velocities away from the pipe wall were flatter than predicted.

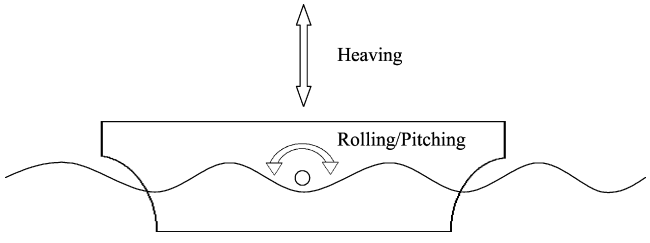

Fig. 1. Types of barge movement due to ocean waves.

These flow fluctuations and additional flow resistance during oscillations are important when heat transfer and two-phase flow effects come into play as indicated by studies on the forced convective heat transfer and the critical heat flux condition in the presence of imposed flow oscillations. Isshiki (1966), Otsuji and Kurosowa (1982, 1983, 1984), Ishida et al. (1990), Ishida and Yoritsune (2002) conducted investigations in different types of reactor geometries with natural and forced circulation systems and reported that the critical heat flux under oscillating flow conditions was considerably reduced. A number of methods of estimating critical heat flux for fixed steam generating tubes are available; extension of these to oscillating flows would require knowledge of the induced flow oscillations (Otsuji and Kurosowa, 1983). Although there have been a number of studies of the flow and pressure drop in an oscillating tube, no reliable method exists to estimate the induced flow rate oscillations. A knowledge of the effect of the various types of oscillations on the flow and heat transfer is very important in the design and operation of equipment for marine applications. This paper describes an experimental investigation of the effect of heaving on the flow in a single vertical tube. Studies (Isshiki, 1966) indicate that the maximum heaving acceleration during ship motion in the Indian Ocean is of the order of 0.1g and with the period of oscillations falling in the range of 3–12 s. In the present study, the effect of heaving acceleration in the range of 0.1–1.125 m/s^2 (equivalent to 0.01–0.115g) with a time period of 2–8 s have been investigated. Details of the experiments and the results obtained are discussed below.

2. Experimental set-up

A mechanical simulator is used to generate the low frequency oscillations in the test section. The test section is fixed onto the framework of the mechanical simulator and moves with it. To maintain structural integrity, the test section is connected to rest of the flow loop with flexible hose connections. A computer-based data acquisition system is used to record the instantaneous position (displacement) of the test section, the flow rate and the pressure drop in the test section.

2.1. Mechanical simulator

An eccentrically mounted connecting rod device (Fig. 2) is used to simulate the low frequency oscillations. The connecting rod is driven by a three-phase motor rotating at a speed of 1440 rpm. A gear reduction system, consisting of two reduction gears, one of a fixed ratio of 100:1 and the other of continuously variable reduction ratio from 6:1 to 1.5:1, and a set of stepped pulleys are used to reduce the speed of rotation to the desired

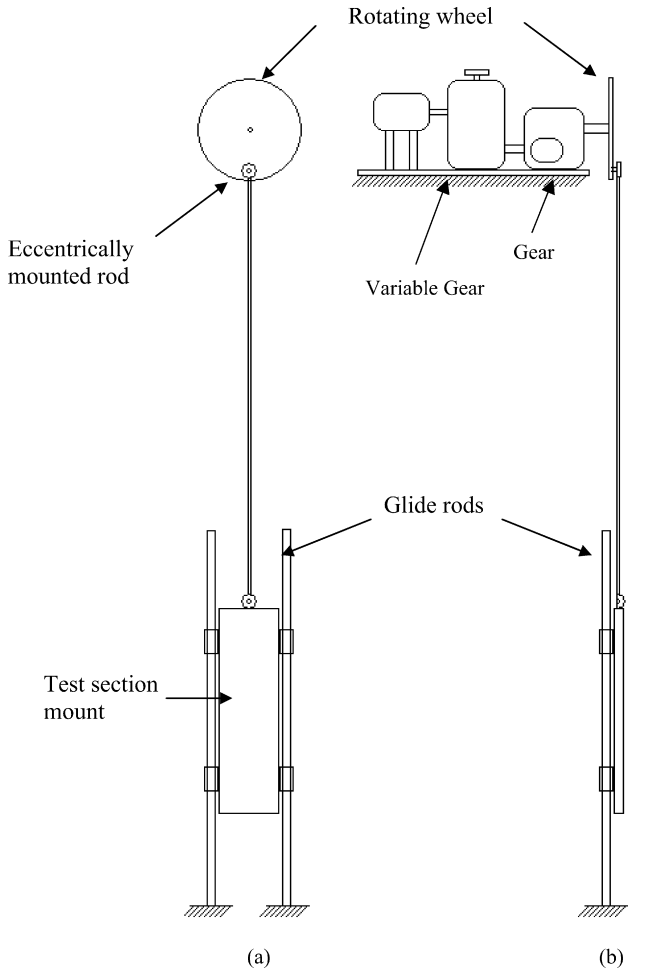

Fig. 2. Schematic diagram of the mechanical simulator: (a) front elevation and (b) side view.

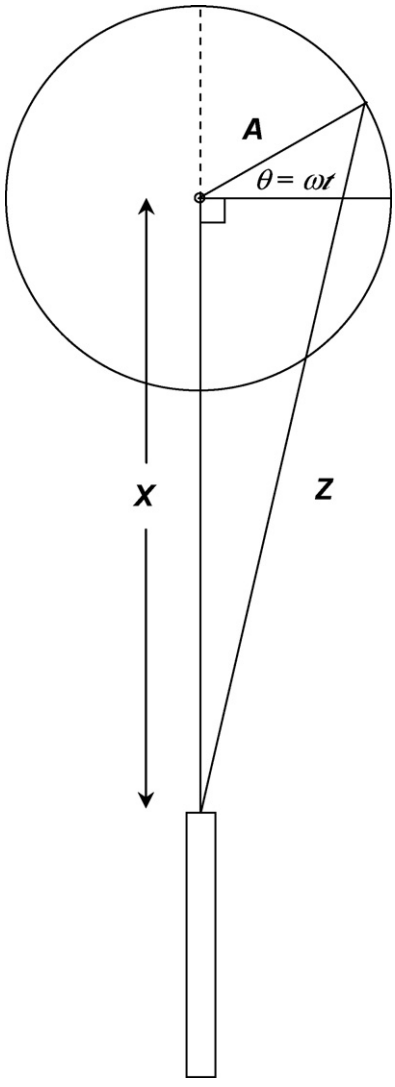

Fig. 3. Kinematics of the mechanical simulator.

range of 8–30 rpm. An eccentric rod type of arrangement converts the rotational movement to vertical movement. The rotating wheel is a metal disk of diameter 0.3 m. The centre of the disk is fixed to the gear shaft and one end of the connecting rod is fixed in a radial slot on the disk. The other end of the connecting rod is fixed to the frame on which the test section is mounted. As the disc rotates, the connecting rod moves up and down and also moves the test section frame. The test section frame slides on two rigid vertical steel guide rods, each of which has one end fixed on the ground.

The mechanical simulator can produce heaving amplitude of up to 0.125 m with a period of oscillation varying from 8 to 30 cycles/min, which is equivalent to an acceleration in the range of 0.1–1.125 m/s^2. The variable reduction gear is used to set the test section oscillation period manually at the desired value. A linear variable displacement transducer (LVDT) is used to track the displacement of test section with time from which the frequency and the time period of oscillations can be found. The LVDT consists of a primary and two secondary coils with a common movable magnetic core. An oscillator excites the primary coil with an alternating current of constant frequency. Consequently, alternating currents are induced in both secondary coils with amplitudes depending on the core position. A displacement of the core yields a higher voltage in one secondary coil and a lower voltage in the opposite coil. The difference between both secondary voltages that are measured is proportional to the displacement.

Displacement of the test section depends on the kinematics of the mechanical simulator whose line diagram is shown in Fig. 3. The displacement can be obtained from the law of cosines

$$X^2 + A^2 - 2XA\cos\left(\frac{\pi}{2} + \theta\right) = Z^2 \tag{1}$$

Solving for X

$$X = A\cos\left(\frac{\pi}{2} + \theta\right) + \sqrt{Z^2 - A^2\sin^2\left(\frac{\pi}{2} + \theta\right)}$$

When $Z \gg A$, X can be written as

$$X = A\cos\left(\frac{\pi}{2} + \theta\right) + Z \tag{2}$$

Therefore, the vertical displacement (x) of the test section is

$$x = X - Z = -A\sin\theta = -A\sin\omega t \tag{3}$$

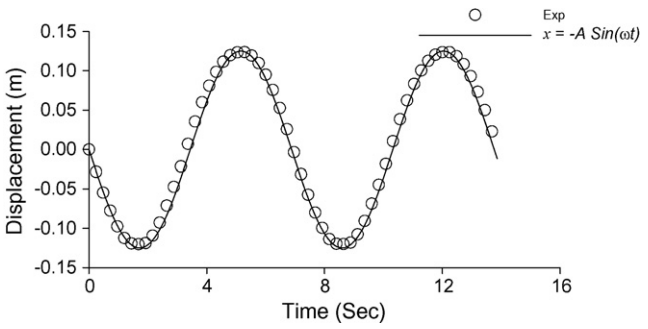

Fig. 4. Typical signal from the LVDT and comparison with a sine curve.

The velocity and the acceleration of the test section can be found by differentiating Eq. (3) once and twice, respectively. The velocity v is

$$v = -A\omega \cos \omega t \tag{4}$$

and the acceleration

$$a = A\omega^2 \sin \omega t \tag{5}$$

The displacement curve obtained from Eq. (3) and the LVDT readings are compared in Fig. 4.

2.2. The flow loop

The schematic diagram of the experimental set up is shown in Fig. 5. The test section consists of a vertical stainless steel tube of 16 mm i.d. and 1.75 m length. The distance between the pressure taps is 0.89 m. The test section is given inlet and outlet connections through horizontal flexible hoses. The test section is mounted on the frame of the mechanical simulator, which can oscillate. A 1.5 hp multistage centrifugal pump is used to pump water from an open storage tank to the test section. A by-pass valve is provided to recycle excess liquid which is pumped back to the storage tank. A needle valve is used to control the flow to the test section and a gate valve is used to control the bypass. Water from the test section is discharged into the sump to avoid feedback oscillations. A thermocouple (K-type) was used to measure the temperature at inlet. All the experiments have been conducted at 30 °C within a range of ±2 °C. The density and viscosity of the fluid have been taken to be those of water at 30 °C at atmospheric pressure.

2.3. Instrumentation

To measure the oscillations from the mechanical simulator, a linear variable displacement transducer (LVDT) is used. The LVDT can track the displacement of the test section with time. An orifice flow meter fixed after the outlet of the pump is used to measure the flow rate. The orifice is connected to a differential

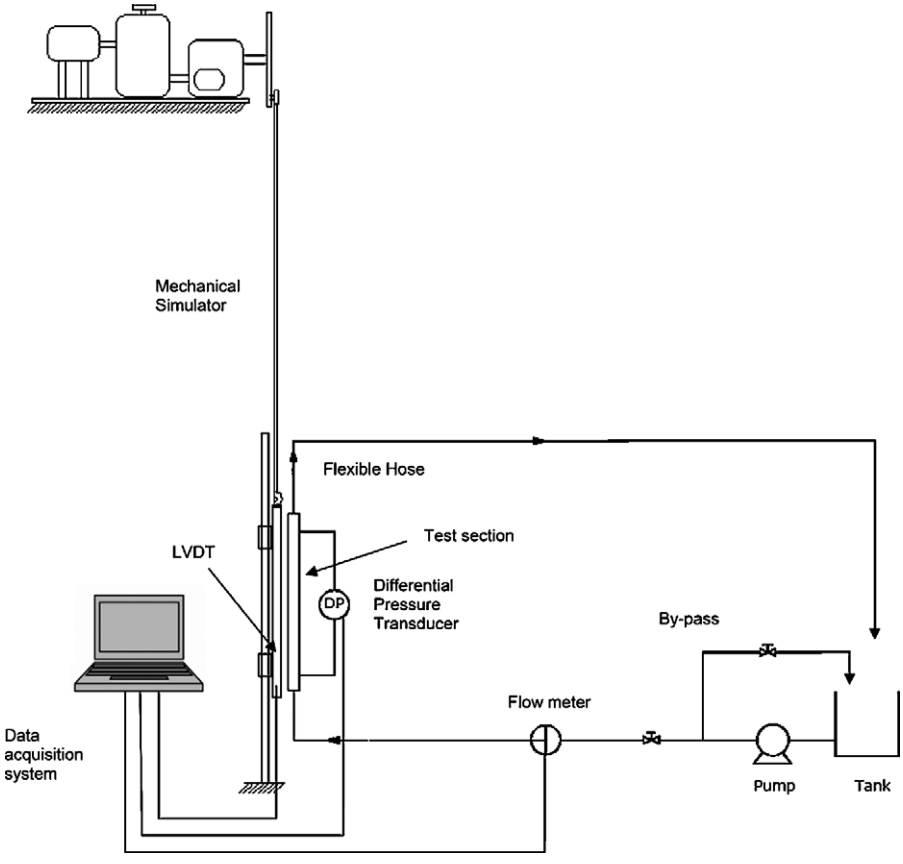

Fig. 5. Schematic diagram of the test loop.

pressure transducer (range 0–0.2 bar) which measures the pressure difference online. Thus, it can measure the fluctuations in the flow rate induced by oscillations. A differential pressure transducer (range 0–0.2 bar) is also used to measure the pressure drop across the test section dynamically. In each case, the pressure taps were connected to the transducer by silicone oil-filled lines; this prevented any damping of the oscillations by compressible volume due to air leakage. A computerized data acquisition system with analog-to-digital (A/D) cards is used to collect the transient data. A data sampling rate of 250 samples per second has been found to offer sufficient resolution of the transients in the frequency ranges of interest. The rig was bench marked by conducting experiments under non-oscillating conditions. The measured pressure drop under laminar and turbulent flow conditions agreed well with theoretical and empirical correlations.

The dynamic response of the instruments depends on the response time. The LVDT's response time is less then 5 ms and the pressure transducer's response time is 55 ms. The orifice is connected to a pressure transducer with response time of 55 ms.

The response time of the instruments is sufficient to track the variation in the parameters of period of oscillations 2–7.5 s. The orifice flow meter is with 5 mm orifice diameter and 16 mm pipe diameter ($\beta = 0.3125$). Quasi-steady theory can be applicable for the flow range studied (Gajan et al., 1992). Square root error in the flow rate is eliminated by converting the instantaneous pressure droops to instantaneous flow rate using the steady state calibration curve.

3. Experimental procedure

3.1. Range of parameters

Experiments have been conducted over a range of oscillation frequencies and flow rates. Oscillation periods were varied from 2 to 8 s for different flow rates. The measured LVDT reading is used to find the different variables, *i.e.*, displacement, velocity, acceleration, period of oscillation and frequency of oscillations. The water flow rate was varied such that the Reynolds number, based on mean flow velocity and the tube inner diameter, varied in the range of 500–6500. The pressure drop fluctuations and the induced flow rate fluctuations were measured for a period of 300 s for each flow condition.

3.2. Experimental uncertainty

The data reduction is based on the measurement of three primary parameters, namely, the displacement from which the frequency, amplitude and thus the effective gravity have been deduced; the pressure drop across the orifice flow meter to measure the (instantaneous) flow rate; and the pressure drop across the test section over a length of 0.89 m. The resolution of the data acquisition system used in the present study is 10^{-4} V. The uncertainty in the measurement of pressure drop is $\pm 0.25\ \mathrm{N/m^2}$. The uncertainty in the measurement of displacement is ± 0.015 mm.

3.3. Data analysis

The highest frequency of imposed oscillations in the experiments is 30 cycles/min. It is possible for high frequency oscillations (vibrations) to appear if the motion of the simulation is not smooth. In order to resolve these and any flow-related higher harmonics which may appear in the measured variables, data sampling is carried out at a sampling rate of 250 Hz which would allow frequencies of 120 Hz to be resolved without aliasing errors. The data analysis has been done using MATLAB. The digital data are smoothened using the Savitzky-Golay filter, which is a digital polynomial filter. Filtering of the signal can eliminate the noise, if any, due to the AC signal of frequency 50 Hz. Using the LVDT signal to identify the beginning of the cycle, the signals corresponding to two cycles from the pressure transducers are extracted and then averaged. These are fitted to sinusoidal curves and the corresponding constants are found. The collected, the filtered and the averaged signals are shown in Fig. 6. The raw signals obtained from LVDT and orifice pressure transducer (converted to Reynolds number) for 50 s are shown in Fig. 6(a). The filtered signal and point that cut the Reynolds number based on displacement curve at every two cycles are shown in Fig. 6(b). The averaged two cycles of displacement curve and corresponding velocity and acceleration are shown in Fig. 6(c). The corresponding averaged Reynolds number and those fitted to a sinusoidal curve also shown in Fig. 6(c).

4. Results and discussion

4.1. Flow rate fluctuations

Direct measurement of the flow rate fluctuations was possible with the dynamic measurement of the pressure drop across the orifice meter. As shown in Fig. 6, the imposed oscillations of the test section induced temporal fluctuations in the flow rate with a predominant frequency corresponding to the imposed frequency. The flow rate response was quantified by finding the amplitude of the sinusoidal curve which fitted the data over two cycles, as shown in Fig. 6. The fluctuating flow rate is converted into a fluctuating Reynolds number and is plotted in Fig. 7 as a function of the mean Reynolds number for various acceleration magnitudes. It can be seen that the dimensionless fluctuating flow rate increases as the magnitude of acceleration increases while keeping the mean Reynolds number constant. The effective acceleration increased as a result of increasing the frequency of oscillation, which is proportional to the square of the frequency of oscillation, and this increases the level of fluctuations in the test section. The consistent variation across a range of effective accelerations and flow rates shows the reproducibility of the results.

Fig. 7 also shows a remarkably consistent variation of the magnitude of the flow fluctuation with mean Reynolds number. The magnitude of the flow rate fluctuations decreases as the mean flow rate increases. This trend is present in both laminar (it is assumed that the transition to turbulence is not affected by the fluctuations) and turbulent flows. The magnitude of flow rate oscillations is relatively high at low flow rates. This effect

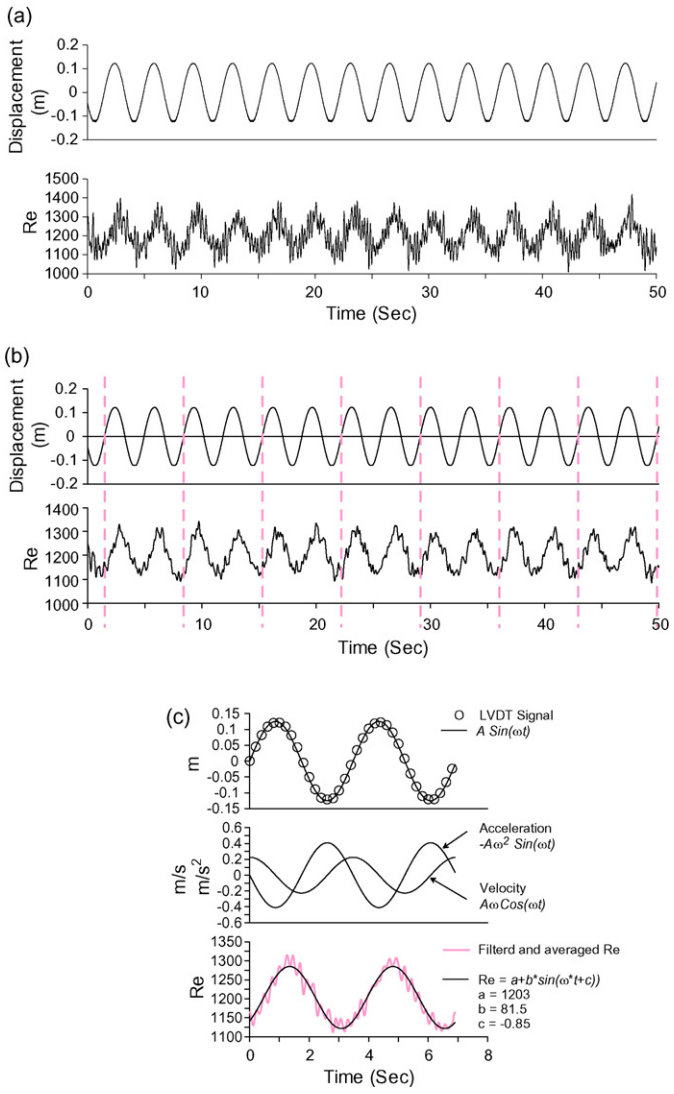

Fig. 6. Analysis of the signals: (a) raw signals obtained from (i) LVDT and (ii) differential pressure transducer measuring the flow rate, (b) filtering of the signals, and (c) averaging and fitting of the signals to a sine curve.

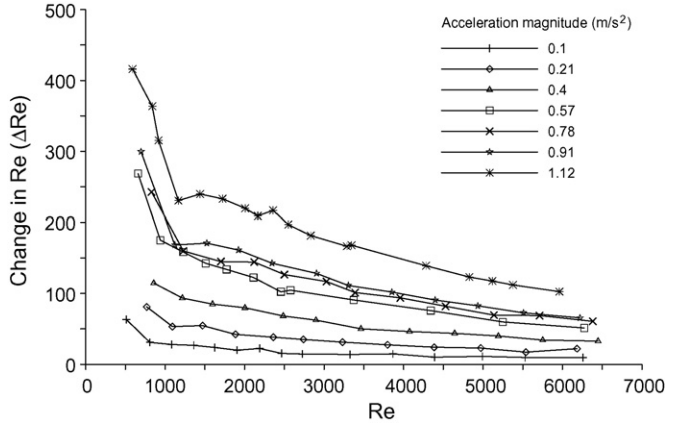

Fig. 7. Variation of the amplitude of induced flow rate fluctuation (ΔRe) with Reynolds number at different acceleration magnitudes.

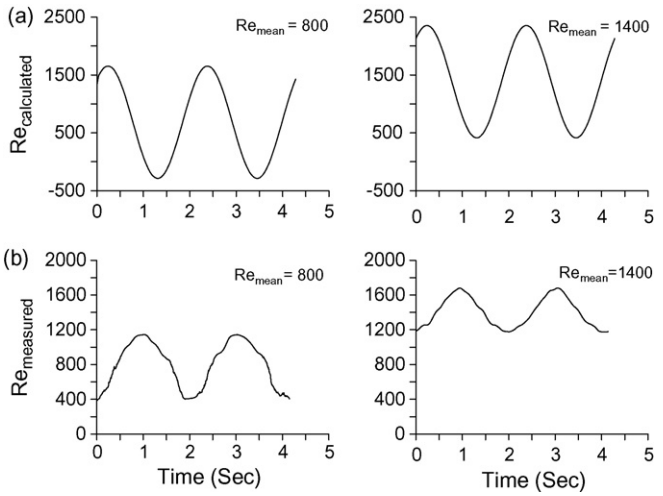

Fig. 8. (a) Theoretical and (b) measured variation of the flow rate for an imposed frequency of 29 cycles per minute at a Reynolds number of (i) 800 and (ii) 1400.

calls for some examination as the theoretical study of Claman and Minton (1977) suggests that, although the local velocity exhibits temporal oscillations and spatial deviations from the parabolic profile under laminar flow, the cross section-averaged flow rate oscillations are independent of mean flow rate. This is illustrated in Fig. 8 where the measured magnitude of flow rate oscillations and the computed magnitude of flow rate oscillations (from the solution for the velocity profile due to Claman and Minton, 1977) are shown for Reynolds numbers of 800 and 1400 for an oscillation frequency of 29 cycles/min. The experimental data shows a clear reduction in the magnitude of the flow rate oscillations while the computed solutions show the same magnitude of flow rate variations at higher mean flow rates. The Reynolds numbers are sufficiently far from the critical Reynolds number of 2100 for pipe flow that both can safely be assumed to be under laminar flow conditions.

The dependence on Reynolds number of the induced fluctuations in the flow rate may be attributed to an entrance length type of effect. The flow in an oscillating pipe can be considered as a combination of two classical problems of fluid mechanics, namely, the flow near an oscillating infinite plate (also called Stokes' second problem, White, 1991) and the Graetz problem of flow development in the entry region of a long pipe (Shah and London, 1978). In the first case, only the fluid near the oscillating plate is affected and shows a periodic variation corresponding to the wall motion. Far away from the plate, the fluctuations are damped out by the viscosity and the fluid stands still. The velocity of fluid particles above the oscillating plate depends on the frequency of oscillation, viscosity, distance from the plate and amplitude of oscillation (White, 1991). The thickness of the oscillating boundary layer depends on the viscosity and frequency of the oscillation. In the present case, the tube length is finite and one must consider the axial development of this oscillating boundary layer. In the case of flow in the entrance region of a tube, the boundary layer development is different from that over a flat plate in that the velocity of the inner inviscid core increases with distance. This has the effect of thinning the boundary layer compared to that for a flow over a flat plate.

Shah and London (1978) recommend the following correlation to estimate the entrance length under laminar flow conditions in a pipe:

$$\frac{x_L}{D} \approx \frac{0.6}{1+0.035Re} + 0.056Re \tag{6}$$

where x_L is the entrance length, D the diameter of pipe and Re is the Reynolds number.

As a first approximation, the development of the oscillating boundary layer in an oscillating tube wall can be likened to the development of the boundary layer in the entrance region. Even though the fluid enters the test section as fully developed, the thickness of the oscillating boundary layer will be small at the entrance to the test section. It will slowly grow downstream and eventually, the oscillating boundary layers from the curved walls meet to give rise to fully developed oscillating flow field in the tube. If this is assumed to be governed by Eq. (6), then the required development length is 28, 56 and 84 diameters for Reynolds numbers of 500, 1000 and 1500, respectively. In the present experiment, the first pressure tapping is located at 27 diameters from the inlet of the test section while the second pressure tapping (connected to the differential pressure transducer) a further 55 diameters downstream or at a distance of 82 diameters from the inlet to the test section. Thus, at a Reynolds number of 500, three-quarters of the test section would be under fully developed pulsating flow condition while at a Reynolds number of 1500, only the last quarter of the test section would be under fully developed pulsating flow condition. This may explain the result shown in Fig. 8 where the induced flow rate fluctuation is less at higher Reynolds numbers.

The situation in turbulent flow is more complicated from a theoretical point of view. Since the effective viscosity in turbulent flow is a function of radial position, closed form solutions for the velocity field are not available either for the oscillating plate case or for the pulsatile flow in a pipe. It is however known that because of higher net momentum diffusivity, the entrance length is much shorter than for laminar flow and is typically of the order of 20 diameters. Thus, it is likely that most of the test section is under fully developed flow conditions. However, it is possible that, due to this higher momentum diffusivity under turbulent flow conditions, only a small region near the wall is affected by the wall oscillation. As the Reynolds number increases, the effective diffusivity increases and the region affected by oscillations becomes smaller leading to smaller flow rate fluctuations. This is consistent with the measurements shown in Fig. 7.

Experiments have shown that the magnitude of flow variation (*i.e.*, the maximum amplitude of flow fluctuation) is a function of effective acceleration and mean flow rate. Dimensionless magnitude of flow variation is defined in terms of fraction of magnitude of flow variation to the mean flow

$$\psi = \frac{\Delta Re}{Re} = \frac{\Delta \bar{v}}{\bar{v}} = \frac{\Delta u}{u} \tag{7}$$

Based on the present data, correlations have been developed for the induced flow rate fluctuations in terms of the Reynolds number and the effective acceleration (α). Due to the different Reynolds number dependence of the induced flow rate fluctuation in laminar and turbulent flow conditions (the transition Reynolds number is assumed to 2100), separate correlations are proposed for the two regimes:

$$\begin{aligned} \psi &= 83000\left(\frac{\alpha}{g}\right)\frac{1}{Re^{1.5}} \quad \text{for } 500 < Re < 2100 \\ &= 58000\left(\frac{\alpha}{g}\right)\frac{1}{Re^{1.75}} \quad \text{for } 2100 < Re < 6500 \end{aligned} \tag{8}$$

The fluid moves under the influence of pressure gradient which acts in the direction of axis and frictional individual layers act on each other which are proportional to the velocity gradient. The imposed oscillations on the pipe wall can cause additional forces to act in the system. These wall oscillations will influence the fluid to oscillate along with the wall. The magnitude of flow fluctuations can be directly proportional to influence of oscillations. The term (a/g) represents the magnitude of oscillations in the correlation. When the flow rate is further increased, the inertial forces dominate the flow in the core of the pipe and may dampen the magnitude of flow fluctuations. The magnitudes of flow fluctuations are inversely proportional to the inertial forces. The inertial forces can be characterized by the Reynolds number. The dependency on the Reynolds number of the magnitude of flow fluctuations in the correlation can be attributed to the inertial forces. On the other hand in turbulent flow the effect of inertial forces are more compared to laminar flow.

The performance of the two correlations is shown in Fig. 9. The agreement between experiment and prediction is with a mean absolute error of 8.5%. The correlations are valid for $Re < 6500$ and $a/g < 0.125$.

4.2. Pressure drop

Since the test section is vertical, the measured pressure gradient contains the gravitational component. The heaving motion in

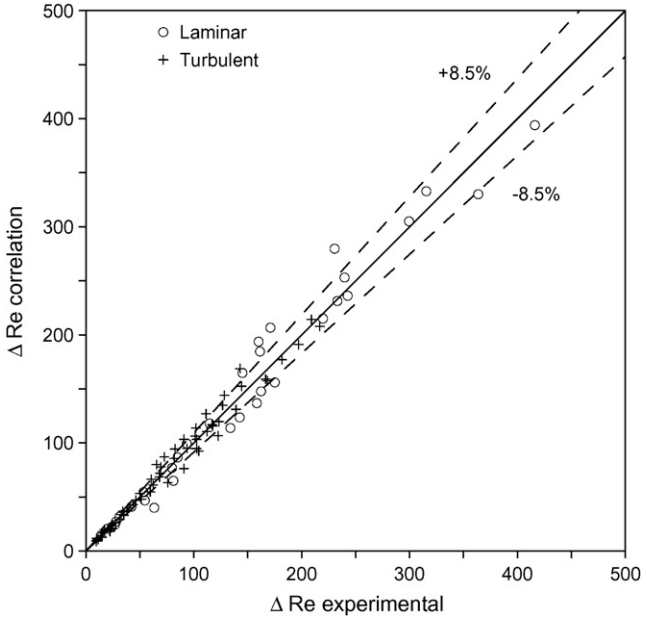

Fig. 9. Performance of the correlation for predicting magnitude of flow rate fluctuation for laminar and turbulent flows.

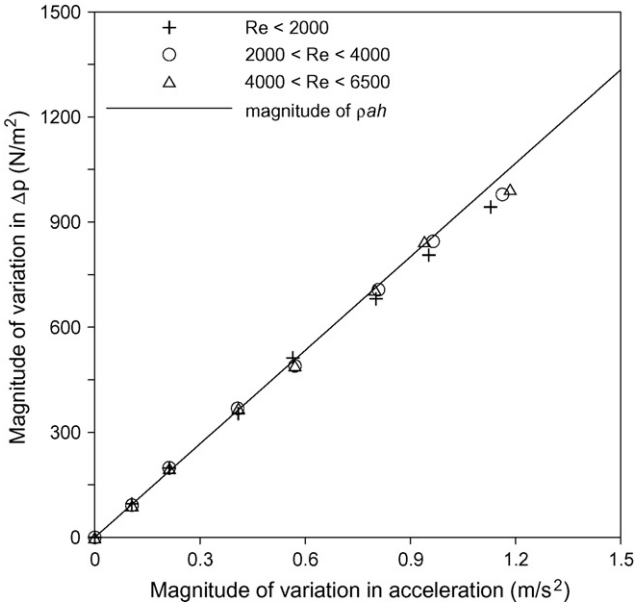

Fig. 10. Measured amplitude of the pressure drop fluctuation as a function of the imposed acceleration magnitude for different Reynolds numbers.

the vertical plane introduces a temporally varying vertical acceleration with a corresponding instantaneous acceleration equal to 'ρh' times of the instantaneous acceleration where h is the height difference between the two pressure taps. The measured pressure gradient therefore would show periodic variation even under no flow conditions. If flow rate fluctuations were induced, then the frictional component too would contribute to the temporal variation in the pressure drop. Fig. 10 compares the magnitude of the variation in the measured pressure drop with the magnitude of acceleration. To facilitate comparison, the flow rates were grouped into three categories: $Re < 2000$, $2000 < Re < 4000$ and $Re > 4000$. It can be seen that the pressure drop variation consists mostly of the acceleration component and very little contribution comes from the flow rate fluctuations. It is only at the highest accelerations do we find significant contribution arising from the flow rate component. The effect of oscillations on the pressure gradient for a given flow rate is summarized in Fig. 11,

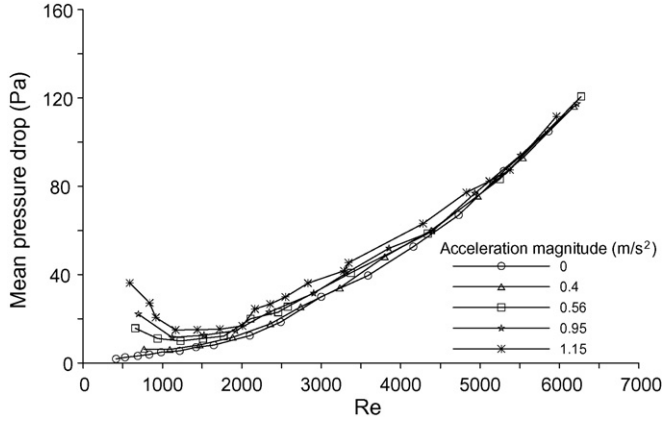

Fig. 11. Variation of the measured mean pressure drop with Reynolds number for different acceleration magnitudes.

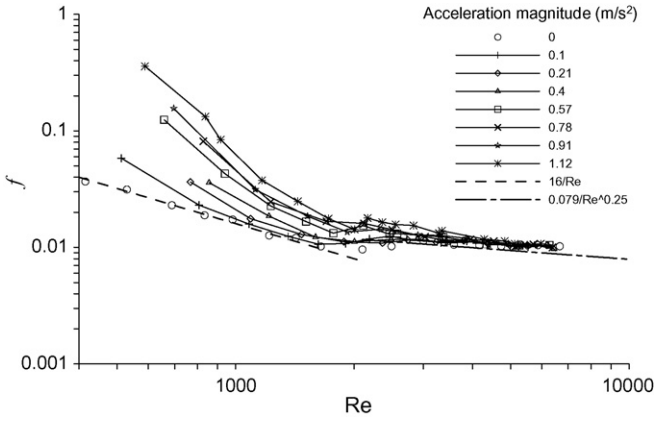

Fig. 12. Variation of the friction factor deduced from the pressure drop measurements with Reynolds number for different imposed acceleration magnitudes.

where the measured mean frictional pressure drop is plotted as a function of the mean Reynolds number based on the mean flow velocity obtained from the time-averaged flow rate. It is clear here that there is a significant and consistent effect of the oscillations on the frictional pressure gradient at low flow rates. As the flow rate increases, the effect of oscillations decreases and becomes negligible at Reynolds numbers greater than around 5000.

The increase in the frictional pressure gradient in pulsatile flows has been reported previously in the literature (Hershey and Song, 1967). Pulsating flow is broadly classified into three regions, namely, quasi-steady, intermediate and inertia dominant regions. The limits of these regions are demarcated by a dimensionless frequency parameter defined as

$$\sqrt{\omega'} = \frac{D}{2}\sqrt{\frac{\omega}{\nu}} \tag{9}$$

where ω is the angular frequency of oscillation and ν is the kinematic viscosity. The flow is quasi-steady for $\sqrt{\omega'} < 1.32$; intermediate for $1.32 \leq \sqrt{\omega'} < 28$ and inertia-dominated for $\sqrt{\omega'} \geq 28$. In the quasi-steady region, the time-averaged friction factor under oscillating flow conditions remains the same as that under steady conditions at the same Reynolds number. In the intermediate and inertia-dominated regions, the mean friction factor is expected to be higher than that for steady flow at the same Reynolds number. In the present study, the dimensionless frequency parameter $\sqrt{\omega'}$ ranges from 7.7 to 13.9 and the flow conditions correspond to those in the intermediate region. This is borne out by the results shown in Fig. 11 where the pressure drop is shown as a function of Reynolds number.

As in the case of the induced flow rate fluctuations, the present results show a strong effect of Reynolds number on the induced excess pressure drop. Using the measured flow rate, the results of Fig. 11 are converted into the equivalent friction factor and are plotted in Fig. 12 as a function of Reynolds number. It is seen that while significant enhancement of the friction factor is present at low Reynolds numbers, very little effect is seen for Reynolds numbers greater than 5000. A correlation has been sought for the excess friction factor due to the oscillations. This

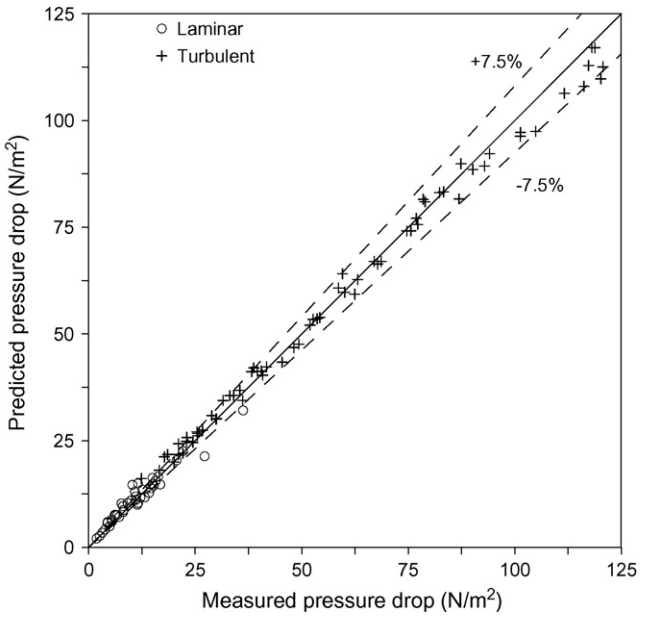

Fig. 13. Performance of the correlation for predicting pressure drop for laminar and turbulent flow conditions.

parameter has been defined as

$$\Delta f = \frac{f_{os} - f_{th}}{f_{th}} \tag{10}$$

where f_{os} is the measured friction factor under oscillating conditions and f_{th} is the theoretical friction factor given by

$$\begin{aligned} f_{th} &= \frac{16}{Re} \quad \text{if } Re < 2100 \\ &= \frac{0.079}{Re^{0.25}} \quad \text{if } Re > 2100 \end{aligned} \tag{11}$$

It is assumed that the Reynolds number for transition to turbulence remains unchanged by the oscillations and that the Blasius formula for friction factor under turbulent flow conditions is valid from $Re > 2100$. Noting that the Reynolds number dependence of the excess friction factor for laminar and turbulent flows is different, the following correlations are proposed:

$$\begin{aligned} \Delta f &= 7.19 \times 10^8 \left(\frac{\alpha}{g}\right) \frac{1}{Re^{2.5}} \quad \text{for } 500 < Re < 2100 \\ &= 1.77 \times 10^7 \left(\frac{\alpha}{g}\right) \frac{1}{Re^{2}} \quad \text{for } 2100 < Re < 6500 \end{aligned} \tag{12}$$

The flow in the oscillating pipe is influenced by the pipe wall and causes flow fluctuations. The fluctuations in the flow causes more shear and can be accounted for by higher friction factor. The flow fluctuations as well as friction factor is proportional to the effective acceleration which represents oscillations. The Reynolds number dependency can be attributed to a lower magnitude of flow fluctuations at higher flow rates.

The performance of the correlations is shown in Fig. 13; the agreement is within a mean absolute error of 7.5%.

4.3. Uncertainty analysis

The relative uncertainties in using the proposed correlations can be estimated using the method due to Moffat (1988). In the present study the measured variables are the pressure drop, displacement and flow rate. The uncertainty in the measurement of displacement is ±0.1%. Therefore, the uncertainty in estimating effective acceleration is ±0.22%. The uncertainty in the measurement of pressure drop is ±0.1%. The measurement uncertainty in flow rate is ±1%. Therefore, the relative uncertainty in the proposed correlation for magnitude of flow fluctuations (Eq. (8)) for laminar flow is ±0.55% and for turbulent flow is ±0.78%. The relative uncertainty in the proposed correlation for excess friction factor (Eq. (12)) for laminar regime is ±2.5% and for turbulent regime is ±2%.

5. Conclusions

The results from the present experiments show that low frequency, externally-imposed periodic oscillations give rise to fluctuations in the flow rate and the pressure drop. For effective accelerations of up to 0.125 g in a tube of 110 diameters length, it has been found that significant flow rate oscillations are present only under laminar flow conditions. The magnitude of the flow rate oscillations is found to decrease as the Reynolds number increases, presumably due to the flow taking a longer distance to develop. In turbulent flow, the magnitude of flow rate oscillations is less pronounced compared to laminar flow. The friction factor under pulsatile conditions is found to increase with increasing acceleration. At high Reynolds numbers ($Re > 5000$), the flow shows a muted response in terms of both flow rate fluctuations and increase in friction factor.

References

Claman, M., Minton, P., 1977. An experimental investigation of flow in an oscillating pipe. J. Fluid. Mech. 81, 421–431.

Gajan, P., Mottram, R.C., Hebrard, P., Andriamihafy, H., Platet, B., 1992. The influence of pulsating flows on orifice plate flowmeters. Flow Meas. Instrum. 3, 118–129.

Gündoğdu, M.Y., Çarpinlioğlu, M.Ö., 1999. Present state of art on pulsatile flow theory part 1: laminar and transitional flow regimes and part 2: turbulent flow regime. JSME Int. J. 42, 384–410.

Gündoğdu, M.Y., Çarpinlioğlu, M.Ö., 2001. A critical review on pulsatile pipe flow studies directing towards future research topics. Flow Meas. Instrum. 12, 163–174.

Hershey, D., Song, G., 1967. Friction factors and pressure drop for sinusoidal laminar flow of water and blood in rigid tubes. AIChE J. 13, 491–496.

Humphries, J.R., Davies, K., 1998. A floating desalination/co-generation system using the KLT-40 reactor and Canadian RO desalination technology. In: Proceedings of Advisory Group Meeting. International Atomic Energy Agency, Vienna, IAEA-TECDOC 1172, pp. 41–52.

Ishida, I., Kusunoki, T., Murata, H., Yokomura, Y., Kobayashi, M., Nariai, H., 1990. Thermal hydraulic behavior of a marine reactor during oscillations. Nucl. Eng. Des. 120, 213–225.

Ishida, T., Yoritsune, T., 2002. Effects of ship motions on natural circulation of deep sea research reactor DRX. Nucl. Eng. Des. 215, 51–67.

Isshiki, N., 1966. Effects of heaving and listing upon thermal hydraulic performance and critical heat flux of water cooled marine reactors. Nucl. Eng. Des. 4, 138–162.

Moffat, R.J., 1988. Describing the uncertainties in experimental results. Exp. Thermal Fluid Sci. 1, 3–17.

Otsuji, T., Kurosowa, A., 1982. Critical heat flux of forced convection boiling in an oscillating acceleration field—I. General trends. Nucl. Eng. Des. 71, 15–26.

Otsuji, T., Kurosowa, A., 1983. Critical heat flux of forced convection boiling in an oscillating acceleration field—II. Contribution of flow oscillations. Nucl. Eng. Des. 76, 13–21.

Otsuji, T., Kurosowa, A., 1984. Critical heat flux of forced convection boiling in an oscillating acceleration field—III. Reduction mechanism of CHF in subcooled flow boiling. Nucl. Eng. Des. 79, 19–30.

Panov, Y.K., Polunichev, V.I., Zverev, K.V., 1998. Nuclear floating power desalination complexes. In: Proceedings of Four Technical Meeting, International Atomic Energy Agency, Vienna, IAEA-TECDOC 1056, pp. 93–104.

Richardson, E.G., Tyler, E., 1930. The transverse velocity gradient near the mouths of pipes in which an alternating or continuous flow of air is established. Proc. Phys. Soc., London 42, 1–15.

Sexl, T., 1930. Uber den von entdeckten Annulareeffekt. Z. Phys. 61, 349–362.

Shah, R.K., London, A.L., 1978. Laminar Flow Forced Convection in Ducts, Advances in Heat Transfer, Suppl. 1. Academic Press, New York.

Uchida, S., 1956. The pulsating viscous flow superimposed on the steady laminar motion of incompressible fluid in a circular pipe. J. Appl. Math. Phys. (ZAMP) 7, 403–422.

White, F.M., 1991. Viscous Fluid Flow, second ed. McGraw-Hill, New York.

Womersley, J.R., 1955. Method for the calculation of velocity rate of flow and viscous drag in arteries when the pressure gradient is known. J. Physiol. 127, 553–563.